

The Fluorescence Behavior and Stability of AgNPs Synthesized by *Juglans Regia* Green Husk Aqueous Extract

Nasrin Paseban, Parinaz Ghadam* and Pouneh S. Pourhosseini

Department of Biotechnology, Faculty of Biological Sciences, Alzahra University, 1993893973, Tehran, Iran.

(* Corresponding author: pghadam@alzahra.ac.ir
(Received: 04 August 2018 and Accepted: 04 December 2018)

Abstract

Particles with the size of 1-100 nm are known as nanoparticles (NPs). The widespread use of silver NPs (AgNPs) makes it familiar in different industries. They have unique properties as a result of their high surface to volume ratio, although aggregation of NPs interferes with their functions. This phenomenon has several side effects on the environment, the amount of which may depend on the stability of AgNPs. Stability of colloids depends on various agents, such as capping agents and environmental conditions, including pH and ionic strength. In this study, the effects of a variety of electrolytes, such as NaCl (10mM), NaNO₃ (10 and 100mM), and Ca (NO₃)₂ (10mM) at different values of pH were investigated on the aggregation of AgNPs synthesized using an aqueous extract of dried *Juglans regia* green husk. In NaNO₃ 10mM pH 9, NPs were more stable than in other media. Therefore, the special optical and electronic properties of AgNPs in such a medium as well as in water were investigated. The UV-visible extinction spectra of AgNPs in both water and NaNO₃ (10 mM, pH 9.0) showed a surface plasmon resonance (SPR) at 445 nm as well as a broad peak at shorter wavelengths (255 nm). The fluorescence emission spectra of AgNPs at different excitation wavelengths in the range of 245-290 nm revealed emission peaks that were red-shifted in the range of 487-580 nm by the increase in the excitation wavelength. This behavior is attributed to the existence of a variety of emission centers with different energy levels.

Key words: Aggregation, AgNPs, Fluorescence, *Juglans regia* green husk.

1. INTRODUCTION

The widespread usage of AgNPs in medical equipment, textiles, cosmetics etc. have the risk of releasing them to the environment, which can impact on the ecosystem and microorganisms [1]. The toxicity of AgNPs in any ecosystems greatly depends on the stability of colloidal silver. The high surface area to volume ratio of the NPs results in high reactivity of them which leads to particle aggregation. There are three mechanisms for the prevention of adherence colloidal particles, consisting of electrostatic repulsion, steric repulsion and both of them [2]. In DLVO theory, colloidal particles are surrounded by a diffuse electrostatic double layer (EDL) and the balance between van der

Waals attraction forces and electrostatic repulsion forces determines the colloidal stability [3]. The magnitude of the electric charge and the thickness of the EDL area are directly related to various factors, including the type of coating as well as the environmental conditions like the pH, ionic strength, and composition of electrolytes [2]. In biosynthesis procedure of NPs, they are coated in one step by biomolecules, which reduces the aggregation of these particles [4, 5, 6].

One interesting area of research in studying AgNPs is their optical and fluorescence properties [7]. It has been discovered that AgNPs display special fluorescence behavior, depending on their

shape, size, solvent, synthesis procedure, etc. [7-10]. Recently, there are various reports of fluorescence from AgNPs, thereby several explanations have been developed [8, 10-15]. However, the exact mechanism and special factors influencing fluorescence of AgNPs are still unclear [8, 9, 13]. Therefore, the comprehensive explanation of some spectral experiments is quite difficult [8].

In this paper, the effect of environmental conditions (various salts and ionic strengths, as well as different values of pH) on the stability of AgNPs is investigated. Then, a detailed study of the fluorescence properties of AgNPs dispersed in water as well as in NaNO₃ (10 mM, pH 9.0) is reported. The excitation was carried out in the range of 245-290 nm, far from the SPR region of the AgNPs.

2. MATERIALS AND METHODS

2.1. AgNPs Synthesis

AgNPs were synthesized using green husk of *J. regia* according to [16]. In brief, 58 ml of boiling distilled water was added to 1.6 g of dried husk powder in a Meyer flask, whose lid was closed by parafilm and the aluminum foil. The flask was then placed in a 100°C water bath for 10 min. Afterwards, the extract was filtered by Whatman paper no. 1. Finally, 150 µl of extract was added to 10 ml AgNO₃ (Merck) solution (1mM). After 24 hours, NPs were centrifuged and washed three times by water and re-suspended in de-ionized water (hereafter, referred to as water).

2.2. AgNPs Analysis

The relationship between SPR peak, hydrodynamic diameter (HDD) and zeta potential of AgNO₃ solution with different environmental conditions, consisting of pH (3, 6 and 9), ionic strength (10 and 100mM of NaNO₃) and electrolytes (NaCl, NaNO₃ and Ca(NO₃)₂) was investigated by a double beam UV-visible spectrophotometer (UV 1800, Shimadzu,

Japan), dynamic light scattering (DLS) (Nanophox90-246V, Germany) and Zeta potentiometer (Malvern Zetasizer nano.zs), respectively.

2.3. Spectrophotometric Analysis

AgNPs were dispersed in water, and 10 mM solution of sodium nitrate (pH 9.0), then sonicated for 10 min (25 W). UV-visible extinction spectra of the AgNPs were recorded at 25 °C, 200-700 nm, on the UV-visible spectrophotometer. With similar samples, fluorescence measurements were carried out at 25 °C using a fluorescence spectrophotometer (Cary Eclipse, Varian, Victoria, Australia). Excitation was done at 245-290 nm, and intrinsic fluorescence measured in the range 230-700 nm. The excitation and emission slits were both 5.0 nm and the scan rate was 600 nm/min. Both the absorption and fluorescence spectra were taken using 1-cm path length quartz cuvettes.

3. RESULTS AND DISCUSSION

3.1. Size Analysis

HDD of AgNPs in water was determined by DLS analysis. Results show that the NPs have a monomodal particle size distribution with the volume mean diameter (VMD) of about 76 nm (Figure 1).

3.2. Stability of AgNPs

3.2.1. Zeta Potential

Zeta potential experiments assess the stability of NPs in aqueous colloids [17]. It shows the electric potential of the NPs at the boundary of the double layer [18]. The magnitude of the zeta potential is predictive of the colloidal stability. Nanoparticles with zeta potential values greater than +20 mV or less than -20 mV are considered as stable colloids [19]. Here, the zeta potential of the NPs is about -17 mV (Figure 2) indicating that the NPs are fairly unstable.

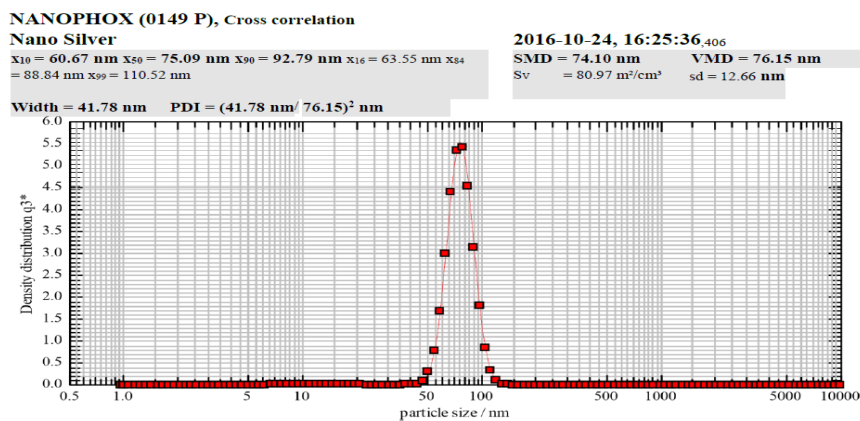


Figure 1. DLS analysis of AgNPs in water.

	Mean (mV)	Area (%)	St Dev (mV)
Zeta Potential (mV): -16.9	Peak 1: -16.9	100.0	6.58
Zeta Deviation (mV): 6.58	Peak 2: 0.00	0.0	0.00
Conductivity (mS/cm): 0.0772	Peak 3: 0.00	0.0	0.00

Result quality : Good

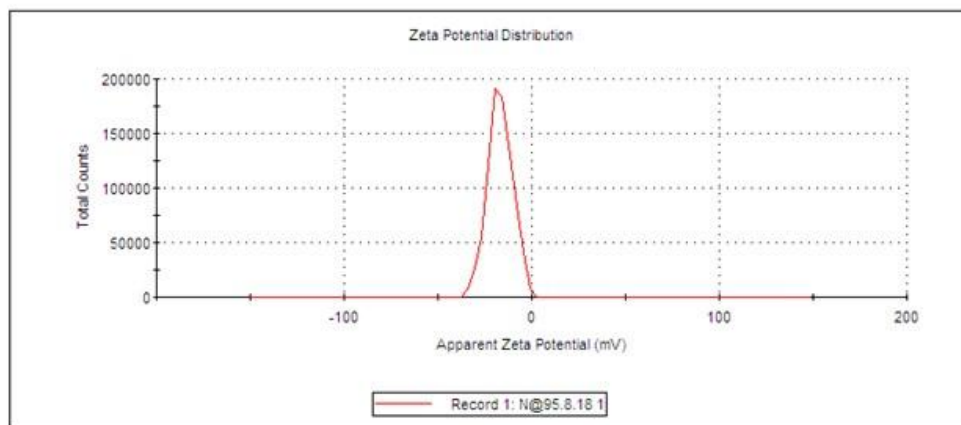


Figure 2. Zeta potential of AgNPs in water.

3.2.2. UV- Visible Spectra Analysis

The SPR peak of AgNPs was investigated at 24 hours as well as two months after the biosynthesis reaction (Figure 3). According to Mie's theory, spherical NPs have only a single SPR band in their absorption spectrum, whereas anisotropic NPs reveal two or more SPR bands, depending on their shape [17]. Figure 3 shows that there is neither difference in the number of nor the shift in the λ_{max} of SPR peaks between the two samples, implying that the shape and distribution of NPs in this period of time are similar. However, there is a small difference in the absorbance amount of the peak tails at 700 nm between the two

spectra. It indicates that the NPs are fairly stable over this time period [9].

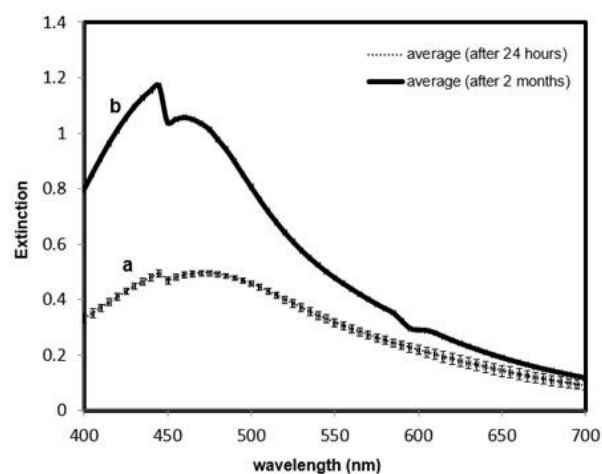


Figure 3. SPR peak of NPs in water, after 24 hours and two months of synthesis.

3.3 The Effect of pH and Ionic Strength on Stability

The influence of electrolyte type, containing cations and anions, on the AgNPs stability was investigated. Thus, Na^+ and Ca^{++} as two examples of monovalent and divalent cations, respectively were chosen. Then, two anions for Na^+ consisting of NO_3^- and Cl^- were selected. The NO_3^- anion for Ca^{++} was also examined. However, the Cl^- anion was not investigated for this cation, because CaCl_2 salt is water-insoluble.

The SPR peak of AgNPs in the presence of different salt solutions, such as Ca

$(\text{NO}_3)_2$ (10 mM), NaCl (10mM) and NaNO_3 (10 and 100mM) at pH 3, 6 and 9 was investigated. The SPR peaks of the NPs in the presence of Ca $(\text{NO}_3)_2$ in the three pH values were extremely weak (Figure 4A), which reveals that the increase of cation valence is not suitable for NP synthesis. Therefore, further investigations were performed on NaCl (10 mM) and NaNO_3 (10 and 100mM) at these pH values (Figures 4 B-E) and Ca $(\text{NO}_3)_2$ electrolyte was not further studied. Also, the zeta potential and HDD of NPs in the presence of these electrolytes were examined (Figures 5 A, B).

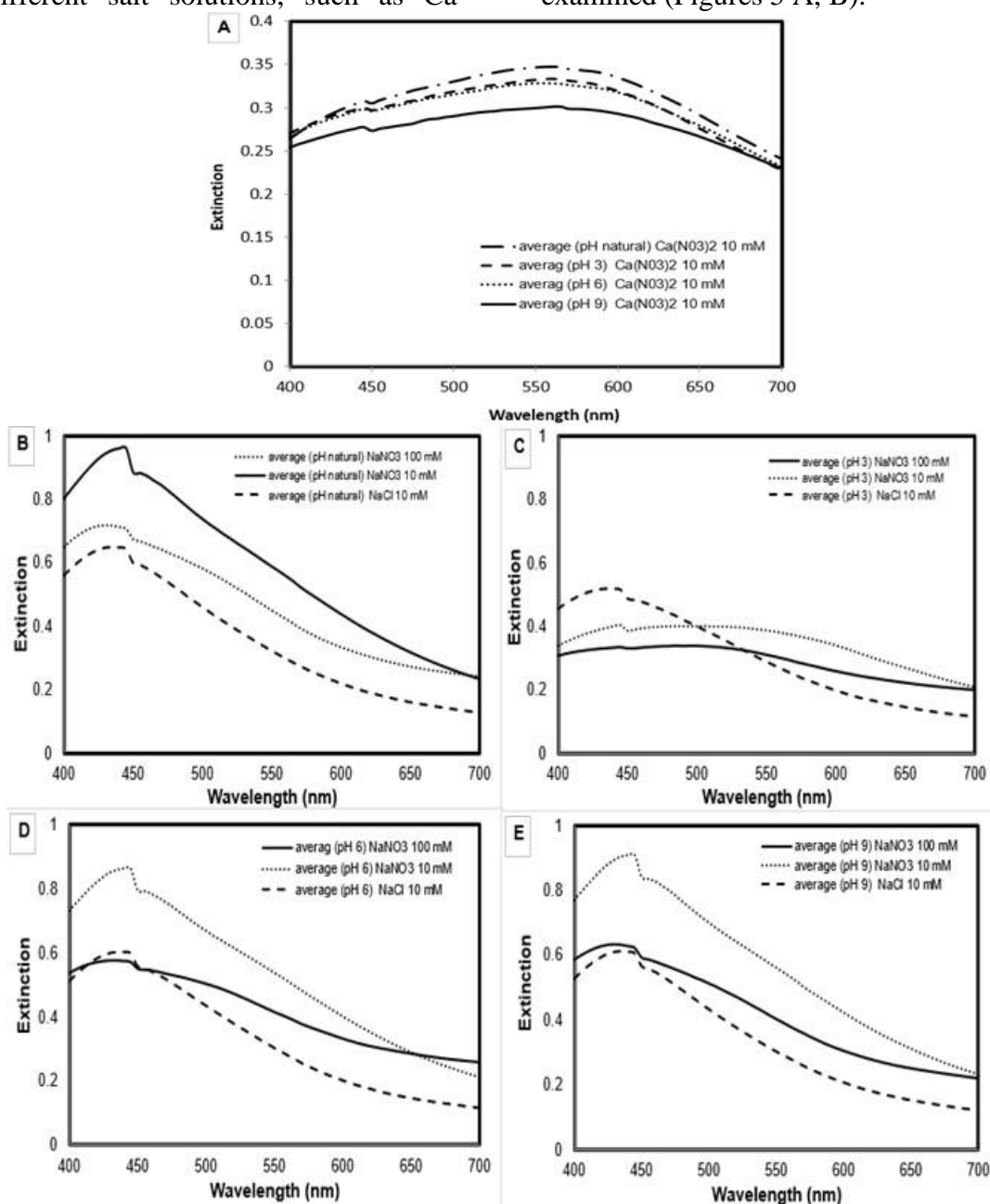


Figure 4. SPR peaks of NPs in the presence of (A) $\text{Ca}(\text{NO}_3)_2$ 10mM in three pH values of 3, 6 and 9, (B, C, D, and E) NaCl 10mM, NaNO_3 10 and 100mM at (B) neutral pH, (C) pH 3, (D) pH 6, and (E) pH 9.

The appearance of negative and positive zeta potential for NPs incubated at pH 3 in NaCl and NaNO_3 respectively indicates that in both media the NPs are unstable (Fig. 5A). When the pH of both electrolytes rises, the NPs become more stable. Results show that the most stable NPs are those incubated at pH 9 in NaNO_3 10mM (Fig. 5A). Previous studies on the zeta potential of NPs coated with citrate, NaBH_4 (Sodium borohydride) and BPEI (Branched Polyethylenimine) have also shown that these NPs are electrostatically stable; hence the stability of them is optimized by changing the ionic strength and pH. On the other hand, the stability of the NPs coated with PVP are sterically stable, therefore the ionic strength and pH changes have not influenced their stability [2]. Here, the results represent that the coating materials existing in the water extract of walnut shell, give a net negative charge on the particles. Therefore, the mechanism of stabilizing NPs is supposed

to be electrostatic. In order to confirm the above conclusion, the effect of electrolyte, ion strength and pH on the size of the NPs (HDD) were also studied. It is found that at pH values of 6 and 9, the HDDs of NPs in the presence of electrolytes NaNO_3 (10, 100 mM) and NaCl (10 mM) are approximately equal (100 to 150 nm). Hence, the kind of anion has no effect on the size of NPs. However, the HDD of the NPs in the presence of the same electrolytes at pH 3 increases steeply (Figure 5B) indicating that the pH is an important factor that influences the size of NPs. Altogether, the results of zeta potential and HDD determinations reveal that the most stable form of the NPs is in the medium of NaNO_3 10mM, at pH 9. Therefore, further studies of absorption as well as emission spectroscopy were performed on AgNPs in such a medium, and then the findings were compared to those in water.

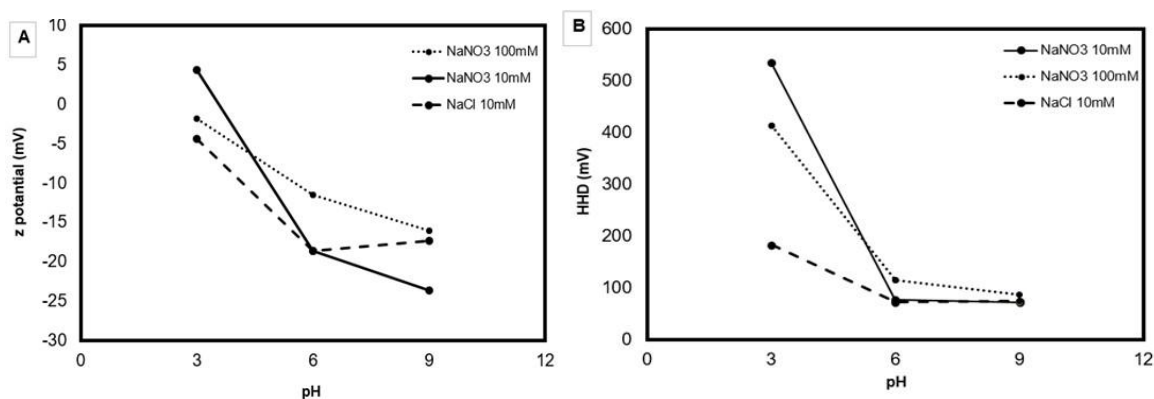


Figure 5. NP stability parameters in different electrolytes at pH 3, 6, and 9 (A) zeta potential (B) HDD.

3.4 Optical Characterization of NPs

Figure 6 (curve a) shows the UV-visible extinction spectra of the AgNPs dispersed in water (extinction = absorption + scattering [9]). It displays a strong extinction peak at 445 nm (blue photons of light), therefore the dispersion appears in

yellowish-brown color. This peak is assigned to surface plasmons, which is characteristic of the AgNPs. The surface plasmon resonance (SPR) peak arises from collective oscillations of valence electrons in the electromagnetic field of the incident light [9, 11, 12, 20]. The position of this

peak, for AgNPs, changes in the range 400-470 nm [7, 8, 10-13, 20-24], depending on the size and shape of the NPs, or dielectric constant of the environment [9, 12, 25, 26]. There is also a broad peak at 255 nm and a rising absorption region towards higher energy with a dent at 210 nm. These peaks are similar to those reported by others and are attributed to the transition of valence electrons to higher energy states [7, 11, 12, 20]. Figure 6 (curve b) shows the spectra of the AgNPs in NaNO₃ (10 mM, pH 9.0). There is no shift in the position of SPR as well as of the higher energy band at 255 nm. However, the absorbance at both wavelengths has decreased. Since the strength of the absorbance at peak reflects the nanoparticle concentration [8, 21], the obtained result indicates that the concentration of the AgNPs in NaNO₃ (10 mM, pH 9.0) decreases, compared with that in water. In addition, the width of the peak can partly show the size distribution of AgNPs [21]. Hence, the similarity of the peak width in both spectra suggests the comparable size distribution of NPs in both media. Furthermore, there are strong absorptions below 230 nm caused by nitrate group [27], which interferes with the dent observed for the NPs in water.

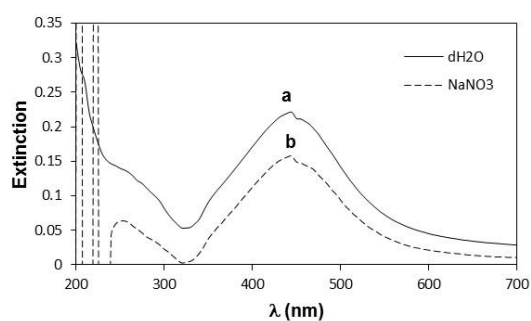


Figure 6. UV-visible extinction spectra of the Ag NPs dispersed in (a) de-ionized water (dH₂O) and (b) NaNO₃ (10 mM, pH 9.0).

Figure 7 shows the fluorescence emission spectra of the AgNPs dispersed in water. Excitation was performed in the range 245- 290 nm, at 5-nm intervals, and

fluorescence measured in the range 230-700 nm. There are two intensive and well-separated peaks for each excitation. The high- intensity peaks from 245 to 290 nm are Rayleigh scattering peaks, positions of which change with the excitation wavelength (λ_{ex}). The intensity of the Rayleigh peaks increases as λ_{ex} increases. The other strong emission peaks appear at 487 nm (a: for λ_{ex} = 245 nm) and shifts towards longer wavelengths (j: 579 nm, for λ_{ex} = 290 nm) with the increase of excitation wavelength. The change in the position of fluorescence peak with excitation wavelength is shown in Figure 8 which shows a linear plot. Here, the fluorescence emission peak intensity gradually decreases with increase of λ_{ex} . It should be noted here that the appearance of the fluorescence emission peak and its interesting behavior, which is red-shifted, are noticed due to the excitation of the AgNPs with a wavelength higher than a threshold value of 230 nm.

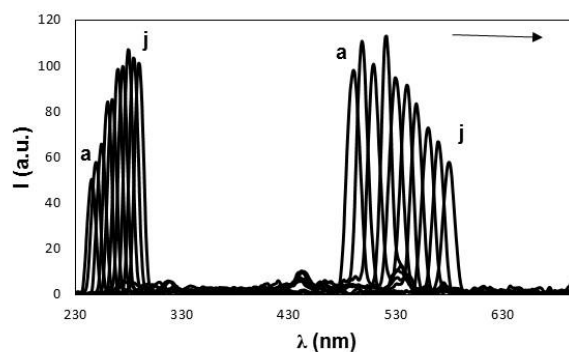


Figure 7. Fluorescence emission spectra of AgNPs dispersed in water. Excitation was carried out at 245 (a), 250 (b), 255 (c), 260 (d), 265 (e), 270 (f), 275 (g), 280 (h), 285 (i) and 290 nm (j). Arrow: the direction of λ_{ex} increase.

The effect of solvent on fluorescence behavior of the AgNPs was investigated by measuring the fluorescence emission of the AgNPs dispersed in NaNO₃ (10 mM, pH 9.0) at similar excitation wavelengths.

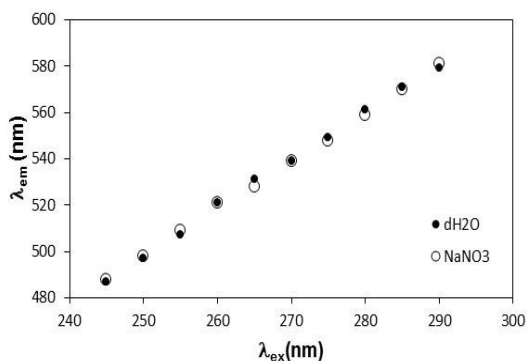


Figure 8. Dependence of emission wavelength on excitation wavelength for Ag NPs dispersed in water and NaNO₃ (10 mM, pH 9.0).

Figure 9 shows the fluorescence emission spectra of the AgNPs dispersed in NaNO₃ (10 mM, pH 9.0). Here too, Rayleigh scattering peaks are appeared at shorter wavelengths in conjunction with fluorescence emission at longer wavelengths.

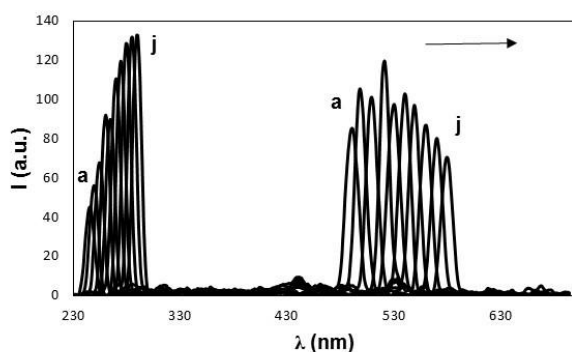


Figure 9. Fluorescence emission spectra of Ag NPs dispersed in NaNO₃ (10 mM, pH 9.0). Excitation wavelengths are as mentioned in Fig. 4 caption. Arrow: the direction of λ_{ex} increase.

Similar trends of intensity changes for both Rayleigh and fluorescence emission peaks, compared to those for the Ag NP peaks in water, are noticed. Furthermore, fluorescence peaks are appeared in similar intensities as for water medium and at similar positions in the range 488-581 nm. The linearity of the change in the emission wavelength with λ_{ex} is as well evident in Figure 8. However, the primary difference

in behavior of the NPs in water with respect to NaNO₃ (10 mM, pH 9.0) is the intensity of the Rayleigh peaks, which is higher in the latter.

In order to determine the exact wavelength of the absorption maxima (λ_{ex}), the excitation spectra of the AgNPs dispersed in water or NaNO₃ (10 mM, pH 9.0) were recorded, according to the method of Siwach et. al [11,12].

Figure 10 shows the fluorescence excitation spectra of the AgNPs dispersed in water (A) for λ_{em} fixed at 487 (solid), 507 (square dot), 539 (long dash dot) and 579 nm (long dash). The spectra are marked by sharp peaks centered at 245, 255, 270 and 290 nm, respectively. This indicates excitation of AgNPs to energy levels corresponding to energy of these peaks. This result is in accord with the fluorescence emission spectra (Figure 7), where maximum emission takes place at these excitation wavelengths. Furthermore, intensity of these peaks is maximum at $\lambda_{ex} = 245$ nm, then decreases as the excitation wavelength increases. This is also in conformity with the fluorescence emission data (Figure 8), previously mentioned.

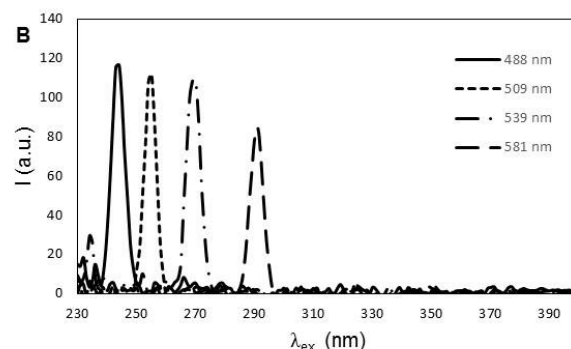
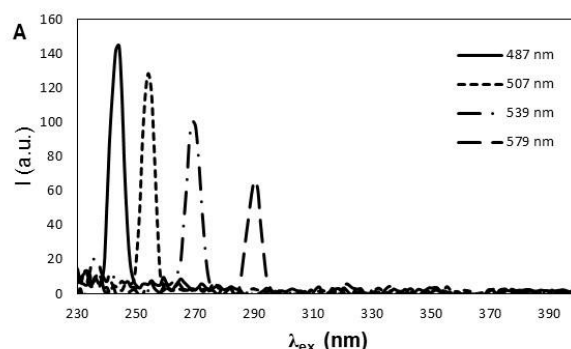


Figure 10. Fluorescence excitation spectra of Ag NPs dispersed in (A) water. λ_{em} was fixed at 487, 507, 539 and 579 nm; (B) NaNO₃ (10 mM, pH 9.0). λ_{em} was fixed at 488, 509, 539 and 581 nm.

The excitation spectra of the AgNPs dispersed in NaNO₃ (10 mM, pH 9.0) (Figure 10B) display sharp peaks centered at 245, 255, 270 and 290 nm for λ_{em} fixed at 488 (solid), 509 (square dot), 539 (long dash dot) and 581 nm (long dash), respectively. This is also corroborated by the fluorescence emission spectra (Figure 9), where intensity of fluorescence peak of AgNPs dispersed in NaNO₃ (10 mM, pH 9.0) is maximum at λ_{ex} = 245, 255, 270 and 290 nm.

Studies on the fluorescence behavior of noble metal NPs have revealed that the position of the fluorescence peak depends on the excitation photon energies. This phenomenon has been considered as a size-selective excitation effect [7]. Thus, the size of the AgNPs is a crucial factor for fluorescence behavior [7, 8, 10]. The explanation of intensity fluorescence

behavior of AgNPs with increase in λ_{ex} observed in this study, i.e. the red shift as well as decrease in the intensity, is proposed as follows.

There are a variety of Ag NP clusters with various size ranges, each has its own energy levels. In other words, there are different emission centers (Figures 11A and B). As the excitation wavelength increases, the photon energy decreases (Figure 11B). Therefore, the electron of those emission centers having lower energy levels are stimulated. Then, relaxation of these electrons emits photons at longer wavelengths. Concomitantly, as the energy of the excitation photon decreases, the transition probability declines, hence the smaller number of fluors (emission centers) is stimulated. Consequently, the smaller number of photons is emitted, resulting in the lower emission intensities. Moreover, the lower the transition probability, the higher the scattering contribution. That is why the intensity of Rayleigh peaks increases gradually as λ_{ex} increases.

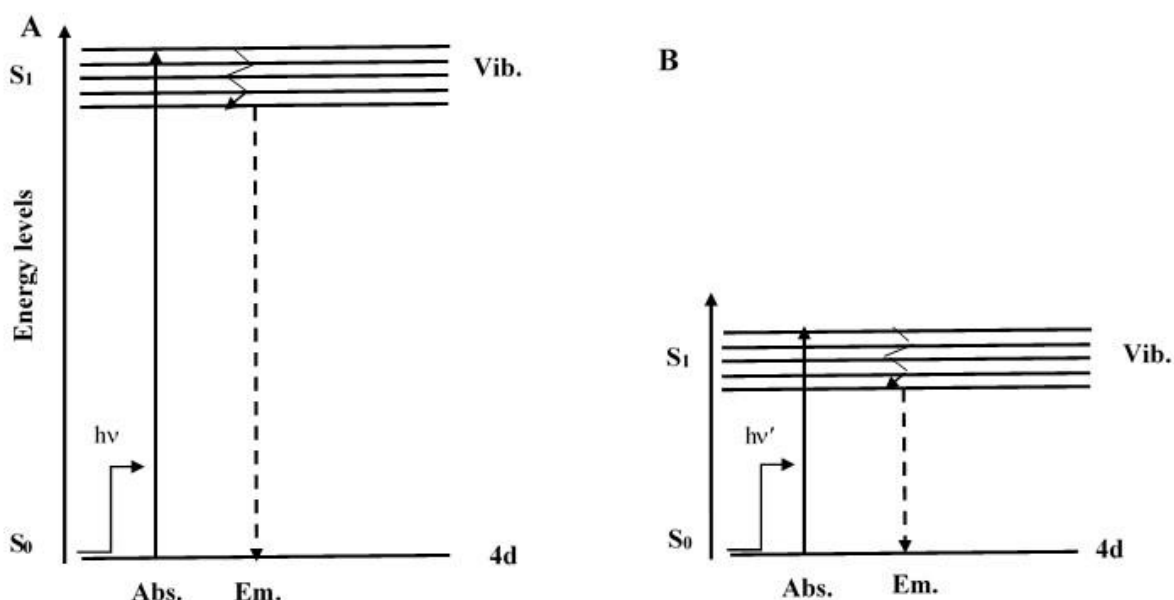


Figure 11. Schematic energy level diagram for emission of Ag NPs. The excitation wavelength has higher energy in diagram (A) than diagram (B). The emitted photon is red-shifted in diagram (B), compared to that in diagram (A). Ex.: Excitation; Em.: emission; Vib.: vibrational levels; S₀: ground state, which is 4d level for Ag⁺; S₁: the first excited state.

$h\nu$ and $h\nu'$: photons stimulating electron from S_0 to S_1 . The energy of $h\nu'$ is less than that of $h\nu$. For simplicity the vibrational levels for S_0 have not been shown.

Altogether, to address the fluorescence behavior of AgNPs, both the size effect (emission peaks) and the surface effect (Rayleigh peaks) should be considered.

4. CONCLUSIONS

In summary, the NPs in aqueous extract of *J. regia* are unstable, while using NaNO_3 (10 mM, pH 9.0) they become more stable. This reveals that the electrostatic repulsion can stabilize the NPs. The extinction spectra of AgNPs in water revealed a strong band in visible region produced by the surface plasmon resonance of the AgNPs. Besides, it showed a broad shoulder in UV region, which was due to the absorption of AgNPs and transition to the excited state. These AgNPs displayed an interesting fluorescence behavior, when excited in the shoulder region. The emission peak linearly shifted towards the red, with the

increase in excitation wavelength. This strange behavior was observed only when the excitation of AgNPs was performed by a wavelength higher than a threshold value of 230 nm. It seems that there are various oligomeric centers of AgNPs with different size ranges. Each cluster has its own energy levels, thus behaves independent of other clusters. Both the optical and fluorescence behavior of AgNPs in NaNO_3 (10 mM, pH 9.0) were similar to those in water.

ACKNOWLEDGMENT

This study was financially supported by the Research council of Alzahra University.

CONFLICT OF INTEREST

There is no conflict of interest.

REFERENCES

1. Keller, A., Wang, H., Zhou, D., Lenihan, H., Cherr, G., Cardinale, B., Miller, R., Ji, Z., (2010). "Stability and Aggregation of Metal Oxide Nanoparticles in Natural Aqueous Matrices", *Environ. Sci. Technol.*, 44: 1962-1967.
2. Badavy, A., Luxton, T., Silva, R., Scheckel, K., Suidan, M., Tolaymat, T., (2010). "Impact of Environmental Conditions (pH, Ionic Strength, and Electrolyte Type) on the Surface Charge and Aggregation of Silver Nanoparticles Suspensions", *Environ. Sci. Technol.*, 44: 1260-1266.
3. Bendersky, M., Santore, M., Davis, J., (2015). "Statistically-based DLVO approach to the dynamic interaction of colloidal microparticles with topographically and chemically heterogeneous collectors", *J. Colloid Interface Sci.*, 449: 443-451.
4. Vinmathi, V., Justin Packia J., (2015). "A green and facile approach for the synthesis of silver nanoparticles using aqueous extract of *Ailanthus excelsa* leaves, evaluation of its antibacterial and anticancer efficacy", *Bull. Mater. Sci.*, 38: 625-628.
5. Singh, A. K., Srivastava, O. N., (2015). "One step Green Synthesis of Gold Nanoparticles Using Black Cardamom and Effect of pH on Its Synthesis", *Nanoscale Research Letters*, 10: 353-365.
6. Sutradhar, P., Saha, M., (2015). "Synthesis of zinc oxide nanoparticles using tea leaf extract and its application for solar cell", *Bull. Mater. Sci.*, 38: 653-657.
7. Basak, D., Karan, S., Mallik, B., (2006). "Size selective photoluminescence in poly (methyl methacrylate) thin solid films with dispersed silver nanoparticles synthesized by a novel method", *Chem. Phys. Lett.*, 420: 115-119.
8. Parang, Z., Keshavarz, A., Farahi, S., Elahi, S. M., Ghoranneviss, M., Parhoodeh, S., (2012). "Fluorescence emission spectra of silver and silver/cobalt nanoparticles", *Sci. Iran., Trans. F*, 19: 943-947.
9. Wiley, B. J., Im, S. H., Li, Z. Y., McLellan, J., Siekkinen, A., Xia, Y., (2006). "Maneuvering the surface plasmon resonance of silver nanostructures through shape-controlled synthesis", *J. Phys. Chem. B.*, 110: 15666-15675.
10. Jian, Z., Xian, Z., Yongchang, W., (2005). "Electrochemical synthesis and fluorescence spectrum properties of silver nanospheres", *Microelectron. Eng.*, 77: 58-62.
11. Siwach, O. P., Sen, P., (2009). "Fluorescence properties of Ag nanoparticles in water, methanol and hexane", *J. Lumin.*, 129: 6-11.

12. Siwach, O. P., Sen, P., (2008). "Synthesis and fluorescence properties of Ag nanoparticles", *Solid State Commun.*, 148: 221-225.
13. Treguer, M., Rocco, F., Lelong, G., Nestour, A., Cardinal, T., Maali, A., Lounis, B., (2005). "Fluorescent silver oligomeric clusters and colloidal particles", *Solid State Sci.*, 7: 812-818.
14. Gill, R., Tian, L., Somerville, W. R. C., Le Ru, E. C., Amerongen, H. V., Subramaniam, V., (2012). "Silver Nanoparticle Aggregates as Highly Efficient Plasmonic Antennas for Fluorescence Enhancement", *J. Phys. Chem. C*, 116: 16687-16693.
15. Zhu, J., Xu, Z. j., Weng, G. J., Zhao, J., Li, J. j., Zhao, J. w., (2018). "Etching-dependent fluorescence quenching of Ag-dielectric-Au three-layered nanoshells: The effect of inner Ag nanosphere", *Spectrochim. Acta, Part A*, 200: 43-50.
16. Abbasi, Z., Feizi, S., Taghipour, E., Ghadam, P., (2017). "Green synthesis of silver nanoparticles using aqueous of dried Juglans regia green husk and examination of its biological properties", *Green Process Synth.*, 6: 477-485.
17. Ajitha, B., Reddy, A., Reddy, P., Jeon, H., Ahn, C., (2016). "Role of capping agents in controlling silver nanoparticles size, antibacterial activity and potential application as optical hydrogen peroxide sensor", *RSC Adv.*, 6: 36171-36179.
18. Shin, H., Yang, H., Kim, S., Lee, M., (2004). "Mechanism of growth of colloidal silver nanoparticles stabilized by polyvinyl pyrrolidone in γ -irradiated silver nitrate solution", *J. Colloid Interface Sci.*, 274: 89-94.
19. Cosgrove, T., (2005) "*Colloid science: Principles, methods and applications*", (Wiley) New Jersey.
20. Siwach, O. P., Sen, P., (2008). "Fluorescence properties of Ag nanoparticles in water", *Spectrochim. Acta, Part A*, 69: 659-663.
21. He, S., Chen, H., Guo, Z., Wang, B., Tang, C., Feng, Y., (2013). "High-concentration silver colloid stabilized by a cationic gemini surfactant", *Colloids Surf. A*, 429: 98-105.
22. Hevus, I., Kohut, A., Voronov, A., (2012). "Micellar assemblies from amphiphilic polyurethanes for size-controlled synthesis of silver nanoparticles dispersible both in polar and nonpolar media", *J. Nanopart. Res.*, 14: 1-11.
23. Jian, Z., Yongchang, W., Yimin, L., (2004). "Fluorescence spectra characters of silver-coated gold colloidal nanoshells", *Colloids Surf. A*, 232: 155-161.
24. Soltanabad, M., Bagherieh-Najjar, M., Kohan Baghkheirati, E., Mianabadi, M., (2018). "Ag- conjugated nanoparticle biosynthesis mediated by Rosemary leaf extracts correlates with plant antioxidant activity and protein content", *Int. J. Nanosci. Nanotechnol.*, 14: 319-325.
25. Abdullah, A., Annapoorni, S., (2005). "Fluorescent silver nanoparticles via exploding wire technique", *Pramana J. Phys.*, 65: 815-819.
26. Olad, A., Ghazjahanian, F., Nosrati, R., (2018). "A facile and green synthesis route for the production of silver nanoparticles in large scale", *Int. J. Nanosci. Nanotechnol.*, 14: 289-296.
27. Edwards, A. C., Hooda, P. S., Cook, Y., (2001). "Determination of nitrate in water containing dissolved organic carbon by ultraviolet spectroscopy", *Int. J. Environ. Anal. Chem.*, 80:49-59.